TABLE I
PENALTIES ARISING FROM EXCESS FILTER BANDWIDTHS FOR A 2.5 GB/S SIGNAL AT BER = 10^{-12} ($B_{EL} = \Gamma_{EL} \cdot (f_B/2)$, $B_{OPT} = \Gamma_{OPT} \cdot f_B$).

		dB penalty (p = 1)		dB penalty (p = 2)	
B_{OPT}(nm)	Γ_{OPT}	Γ_{EL} = 1.0	Γ_{EL} = 1.5	Γ_{EL} = 1.0	Γ_{EL} = 1.5
0.02	1	0.58	2.24	0.80	2.42
0.1	5	1.20	2.77	1.62	3.12
0.4	20	2.15	3.58	2.80	4.16

TABLE II
PENALTIES ARISING SOLELY FROM A FINITE EXTINCTION RATIO

Extinction Ratio	1/(Ext.Ratio)	dB penalty
0.01	100	0.96
0.1	10	3.7
0.25	4	7.0

CONCLUSION

Novel analytical expressions for the receiver sensitivity of optically preamplified systems and penalties arising from nonideal system parameters, have been presented. For the first time, an explicit analytical expression covering the combined effects of APD noise, receiver circuit noise, finite extinction ratio, electrical and optical filter bandwidths, amplifier noise and input coupling loss is given. The effect of various system parameters on receiver performance has been elucidated on the basis of these equations.

ACKNOWLEDGMENT

The permission of the Director of Research, Telecom Australia Research Laboratories, to publish this letter is hereby acknowledged.

REFERENCES

[1] R. G. Smith and S. D. Personick, "Receiver design for optical fiber communication systems," in *Topics in Applied Physics*. vol. 39, Berlin: Springer-Verlag, 1982.
[2] N. A. Olsson, "Lightwave systems with optical amplifiers," *J. Lightwave Technol.*, vol. 7, pp. 1071–1082, 1989.
[3] S. Ryu *et al.*, "Long-haul coherent optical fiber communication systems using optical amplifiers," *J. Lightwave Technol.*, vol. 9, pp. 251–260, 1991.
[4] P. S. Henry, "Error-rate performance of optical amplifiers," *Opt. Fib. Commun. Conf.* 1989, Tech. Digest Series 1989, vol. 5, paper THK3, p. 170.
[5] D. Marcuse, "Derivation of analytical expressions for the bit-error probability in lightwave systems with optical amplifiers," *J. Lightwave Technol.*, vol. 8, p. 1816, 1990.
[6] ——, "Calculation of bit-error probability for a lightwave system with optical amplifiers and post-detection Gaussian noise," *J. Lightwave Technol.*, vol. 9, p. 505, 1991.
[7] I. Jacobs, "Effect of optical amplifier bandwidth on receiver sensitivity," *IEEE Trans. Commun.*, vol. 38, p. 1863, 1990.
[8] R. C. Steele *et al.*, "Sensitivity of optically preamplified receivers with optical filtering," *IEEE Photon. Technol. Lett.*, vol. 3, p. 545, 1991.
[9] P. A. Humblett and M. Azizoglu, "On the bit rate of lightwave systems with optical amplifiers," *J. Lightwave Technol.*, vol. 9, p. 1576, 1991.

100 GHz Wafer Probes Based on Photoconductive Sampling

M. D. Feuer, S. C. Shunk, P. R. Smith, M. C. Nuss, and H. H. Law

Abstract—**We have fabricated optoelectronic wafer probes with both free-space and fiber-optic input, and adapted microwave error correction techniques to enable calibrated measurements with the new probes. Photoconductive switches on the probe tip define stimulus pulses and sampling intervals, and signals are transferred to and from the wafer under test by coplanar waveguide transmission lines and plated contact bumps. Vector error correction eliminates the need for time gating to separate the input and reflected pulses, while enhancing accuracy. Since probe flexure under contact significantly disturbs alignment of free-space beams, fiber-optic input yields the most precise measurements. We demonstrate calibrated, on-wafer, measurements of the complex reflection coefficient S_{11} at frequencies up to 100 GHz.**

Manuscript received October 5, 1992; revised November 20, 1992.
M. D. Feuer, S. C. Shunk, and M. C. Nuss are with AT & T Bell Laboratories, Holmdel, NJ 07733.
P. R. Smith and H. H. Law are with AT & T Bell Laboratories, Murray Hill, NJ 07974.
IEEE Log Number 9207568.

INTRODUCTION

WAFER probing at high speed has revolutionized research, development, and production of high-speed devices. Microwave wafer probes based on transitions from coaxial lines to coplanar waveguide (CPW) are connected to vector network analyzers to provide error-corrected, broadband, S-parameter measurements up to 60 GHz. Waveguide-based probes are available to cover V-band (50–75 GHz), but the cost and complexity of extending the waveguide system to multiple bands are very high.

Optoelectronic (OE) testing driven by picosecond or femtosecond laser pulses offers a broad-bandwidth alternative to conventional, purely electronic systems. Typical OE setups use wirebonds or beam leads to connect external photoconductors to the device under test (DUT) [1]–[4], or use integral photoconductors and transmission lines fabricated as part of the test wafer [5]. With the former approach, wafers cannot be measured whole, throughput is very limited, and vector error correction (accuracy enhancement) is not practical. The latter approach requires additional processing steps, may not be compatible with all substrates, consumes space on the test wafer, and relies heavily on the uniformity of the photoconductive gaps and calibration standards fabricated on each wafer.

To overcome these limitations, we have put the OE conversions onto a probe tip which can be moved to contact various sites on a wafer, as sketched in Fig. 1(a). Besides the obvious benefit to throughput, this approach can be used on whole or part wafers of any material, and permits vector error correction. Recalibration of the system is not needed each time the probe is moved to a new device. Our apparatus is similar to that of Scheuermann *et al.* [6], but we have added fiber-optic input, frequency domain analysis, error correction and independent bias of the DUT and the stimulus gap.

Error correction, based on the measurement of known standard devices, is critical to accurate high-speed vector measurements. Microwave network analyzers depend on it to control the reflections, loss, dispersion and delay due to connectors, discontinuities, aging, and simply the nonideality of real, physical transmission lines, directional couplers and samplers. Although some of these sources of measurement error can be reduced by the simplicity and compact size of an OE test set, they are not eliminated. Also, error correction holds an added advantage for OE systems: it can provide directionality for the test set, eliminating the need for time gating or directional couplers, as discussed below.

Fabrication and Measurements

The probe tips were fabricated from commercial silicon-on-sapphire wafers which were 250 μm thick and had 0.6 μm of undoped epitaxial Si. CPW lines were defined in 0.5 μm gold films by photolithography, and the Si epi was removed from the open spaces by reactive ion etching. The epilayer was left in the photoconductive gaps, which measured 5 by 30 μm, and its carrier lifetimes were reduced into the sub-picosecond range by damage from an implant of 2×10^{14} Si^+ ions at an energy of 300 keV.

The central CPW line comprised a 78 μm center conductor and 39 μm spaces, and stimulus and sampling gaps were placed symmetrically, approximately 1 mm from the tip, as shown in Fig. 1(b). Bias to the gaps was provided by CPW lines similar to the signal line, and both bias and signal lines were terminated in 50 Ω coaxial connectors to minimize back reflections. The three lithographically-defined contact bumps were spaced 150 μm center-to-center and measured 90 μm wide by 340 μm long by 39 μm thick, comprising 35 μm of nickel with a 4 μm gold overlayer for corrosion protection and low contact resistance. The contact bumps had a height deviation of < 3 μm.

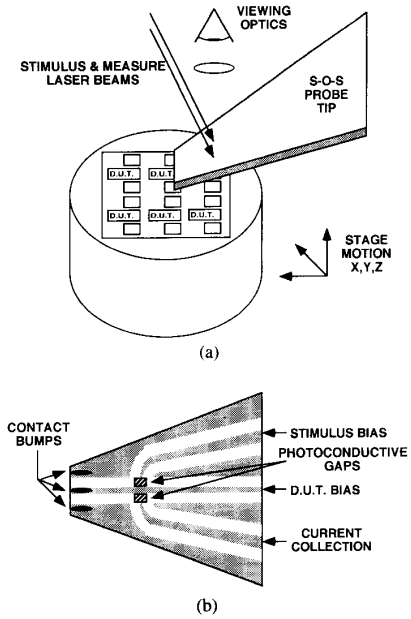

Fig. 1. Schematic layout of optoelectronic wafer probe setup. The system provides high bandwidth, throughput and accuracy.

For the fiber-input probe, single-mode fibers with 80 μm cores were cleaved and bonded to the top (back) surface of the sapphire probe.

Optical pulses at a wavelength of 800 nm were generated by a commercial Ar-pumped, mode-locked Ti-sapphire laser. Pulses from this system are typically 100 femtoseconds long, with a repetition rate of 82 MHz and an average power of ~ 1 W. For the free-beam-input experiments, the optical power was reduced to 25 mW per gap, while the power coupled into each fiber for the fiber-input probe was ~ 10 mW. A variable optical delay was used to sweep the relative delay of the sampling pulses, and the stimulus beam was mechanically chopped to enable lock-in detection, eliminating signal due to dark current leakage in the gaps.

The general methods of photoconductive stimulus/sampling have been discussed by Auston [7]. In brief, we applied a 10 V dc bias to the stimulus gap and monitored the average current from the sampling gap, adjusting the relative delay between stimulus and sampling to obtain the signal voltage versus time.

Results

Fig. 2 shows the time-domain response of the free-beam input probe with various terminations. The incident pulse, a cross-correlation of the electrical stimulus and sampling intervals, has roughly symmetric rise and fall times, with a

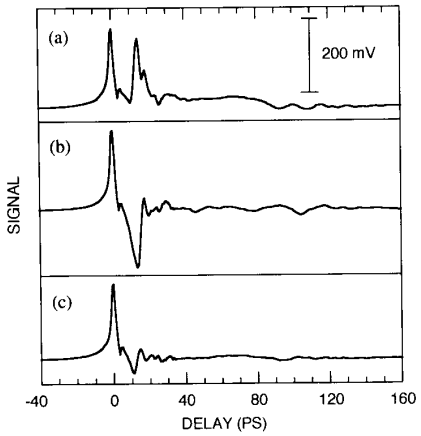

Fig. 2. Time response of optoelectronic wafer probe with free-beam input, contacting different terminations. (a) Probe open in air; (b) probe shorted on gold thin-film bar; and (c) probe on 50-Ω calibration resistor.

width (FWHM) of 2.8 ps. The average stimulus current was ~2.1 μA, implying a pulse voltage of about 450 mV. Fig. 2(a)–(c) show the responses for an open circuit (tip suspended in air), short circuit (tip contacting a bar-shaped gold metallization on the wafer under test), and a 50 Ω load standard (tip contacting the metallized pads of a thin-film resistor), respectively. The latter two terminations are on a calibration tile made for conventional microwave probes by Cascade Microtech. As expected, the open circuit shows a large positive reflection, the short circuit shows a large negative reflection, and the load device shows a much smaller residual reflection due to impedance and mode matching errors at the contact point. In each case, the main reflection signal has an asymmetric shape due to the summation of many components from the finite-length contact bumps and DUT, and small features due to multiple reflections and back reflections are noticeable out to ~120 ps.

To examine reproducibility, each device was reprobed after ~1 h of probing other devices. The major variation observed with the free-beam input probe was a scaling error, due to shifting position of the photoconductive gaps as the probe tip flexed under load. After scaling each curve to normalize the height of the incident pulse, the reflected pulse showed variations in other parts of the curve up to ~4% of the incident peak height (−28 dB). This signal was not random noise, which was present at the level of about 0.05% (−66 dB), but variations of the reflected signal due to changes in the beam, probe position or substrate contact. The fiber-input probe showed no sensitivity to minor probe flexure, but there are still run-to-run variations of ~1–2%, well above the noise floor.

Analysis and Error Correction

Although time-domain responses can be useful in their own right, many design applications require accurate S-parameter data in the frequency domain. In typical calculations of the complex reflection coefficient S_{11} [2]–[4], the incident and reflected pulses are separated by time-window gating, then Fourier transformed and ratioed to obtain the value of S_{11}. A simple propagation factor is used to displace the reference plane to the DUT. This approach has some limitations. Reflections at wirebonds or probe contact points cannot be excluded. The time gate window must be much longer than the input pulse, so the sampling point must be distant, which increases the delay, dispersion, and loss. Reflections from the back end of the test set must be excluded by a separate time gate, limiting the maximum sampling time. Frankel *et al.* [4] have noted that this limited sampling time can interfere with measurements of active devices with long time constants.

Vector error correction techniques can deal with all of these errors, and more, while eliminating the need for time gating. By measuring an open circuit, short circuit, and load device with accurately known properties, one can establish three reference points in the S_{11} plane, to uniquely define the conformal transformation associated with the errors and non-idealities of the test set [8], [9]. The calibration removes all linear errors which are local in frequency and repeatable from run to run, even a directivity error of unity (no directional sensitivity at all). This is why time gating is not needed: the incident signal has been extracted from the measurement of the standard devices. The overall effect of error correction is to place the burden of accuracy on the standard devices, demanding only reproducibility from the test equipment.

To demonstrate the effectiveness of error correction in OE probing, we have measured the reflection from a 12.6-Ω thin-film resistor, and calculated S_{11} over the frequency range from dc to 100 GHz. Since it is small and simple, the resistor should be nearly ideal, appearing at the point $-0.60 + j0.0$ on the Smith chart for all frequencies tested. Fig. 3(a) shows the S_{11} of the test resistor obtained by the time-gated method outlined above, with the time window for the incident pulse set from −32 ps to +4 ps, and the reference plane displacement set at 13.6 ps. The points are scattered loosely about the ideal value, with $S_{11} = -0.57 \pm 0.24 + j(-0.04 \pm 0.18)$ over the frequency range. However, the dc value is actually the wrong sign, clearly demonstrating the importance of systematic errors. Neither adjustment of the time window, nor inclusion of loss or monotonic dispersion in the propagation correction, can improve the result.

Vector error correction, however, makes a substantial improvement, as shown in Fig. 3(b). The short, open, and load terminations shown in Fig. 2(a)–(c) were used. Specifications of the short and load standards were those supplied with the calibration tile, while the open-circuit capacitance, which varies slightly with probe geometry, was set to −18 fF by inspection of the calibrated curves. The error-corrected S_{11} data show less than half the scatter observed when using the time-gating method, with $S_{11} = -0.60 \pm 0.08 + j(0.01 \pm 0.11)$. The remaining discrepancies are due to run-to-run variations which cannot be corrected out.

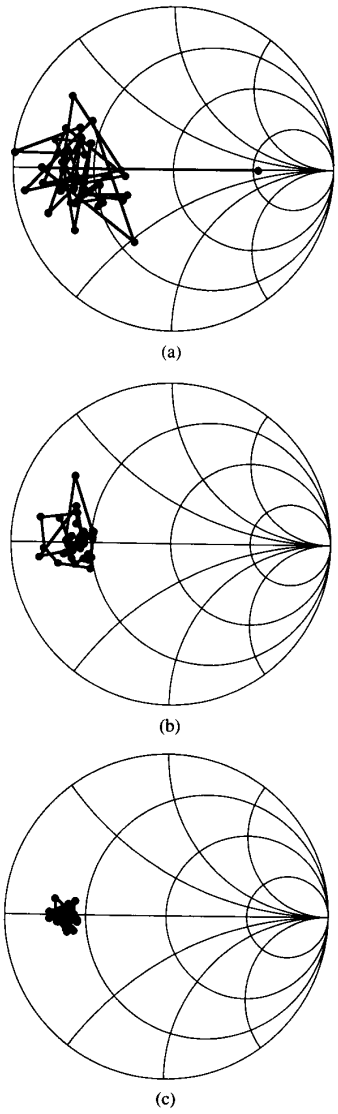

Fig. 3. S_{11} of a thin-film resistor with a dc resistance of 12.6 Ω, from dc to 100 GHz at 2.5 GHz intervals. (a) Data from free-beam input probe, analyzed by conventional time-gating method, shows both systematic and irreproducible errors. (b) Data from free-beam input probe, analyzed by vector error correction, contains only the irreproducible errors. (c) Data from the fiber-input probe, analyzed by vector error correction, shows the best accuracy.

Fiber-optic input to the probe improves reproducibility, yielding the error-corrected measurements shown in Fig. 3(c). A tight distribution of values is observed: $S_{11} = -0.63 \pm 0.04 + j(0.01 \pm 0.04)$ over the 100 GHz frequency range. The remaining scatter in the data is still much larger than the true noise floor, so further gains in reproducibility should bring better system performance. This level of precision will more clearly reveal fine structure of the DUT characteristics, and better calibration standards and methods may become needed to keep the accuracy in line with the precision.

Summary

For the first time, we have obtained on-wafer measurements of S_{11} with full vector error correction over the range from dc to 100 GHz. Error correction, which shifts the burden of accuracy to known standard devices, was shown to improve the precision of device measurements, while it eliminated the need for time-window gating. Optoelectronic probe tips with free-space and fiber-optic inputs were compared, and fiber-optic probes demonstrated superior reproducibility and precision. A two-probe setup will enable measurement of all four two-port S-parameters, and refinements to the standard devices and calibration procedures should yield even better accuracy and wider bandwidth.

Acknowledgment

The authors wish to thank F. Beisser, A. Borges, K. F. Brown-Goebeler, B. Tell, and J. A. Zembas for experimental contributions, J. Wiesenfeld for valuable discussions, and T. Koch for continuing support.

References

[1] P. R. Smith, D. H. Auston, and W. M. Augustyniak, "Measurement of GaAs field-effect transistor electronic impulse response by picosecond optical electronics," *Appl. Phys. Lett.*, vol. 39, pp. 739–741, 1981.

[2] D. E. Cooper and S. C. Moss, "Picosecond optoelectronic measurement of the high-frequency scattering parameters of a GaAs FET," *IEEE J. Quantum Electron.*, vol. QE-22, pp. 94–100, 1986.

[3] M. Matloubian, S. E. Rosenbaum, H. R. Fetterman, and P. T. Greiling, "Wide-band millimeter wave characterization of sub-0.2 micrometer gate-length AlInAs/GaInAs HEMT's," *IEEE Microwave Guided Wave Lett.*, vol. 1, pp. 32–34, 1991.

[4] M. Y. Frankel, J. F. Whitaker, and G. A. Mourou, "Optoelectronic transient characterization of ultrafast devices," *IEEE J. Quantum Electron.*, vol. QE-28, pp. 2313–2324, 1992.

[5] S. L. Huang, E. A. Chauchard, C. H. Lee, T. T. Lee, H-L. A. Hung, and T. Joseph, "On-wafer testing of MMIC with monolithically integrated photoconductive switches," in *IEEE MTT-S Int. Microwave Symp Dig.*, 1992, pp. 661–664.

[6] M. Scheuermann, R. Sprik, J.-M. Halbout, P. A. Moskowitz, and M. Ketchen, "Ultra-High Bandwidth Detachable Optoelectronic Probes," in *OSA Proc. Picosecond Electron. Optoelectron.*, vol. 4, T. C. L. G. Sollner and D. M. Bloom, Eds. Optical Society of America, Washington, DC, 1989, pp. 22–26.

[7] D. H. Auston, "Ultrafast optoelectronics," in *Ultrashort Laser Pulses and Applications*, W. Kaiser, Ed. Berlin: Springer-Verlag, 1988.

[8] J. Fitzpatrick, "Error models for systems measurement," *Microwave J.*, pp. 63–66, May 1978.

[9] I. Kasa, "Closed-form mathematical solutions to some network analyzer calibration equations," *IEEE Trans. Instrument. Meas.*, vol. IM-23, pp. 399–402, 1974.